Accuracy of Green's function estimation from correlation of diffuse elastic waves on thin plates

Lynda Chehami, Emmanuel Moulin, Julien de Rosny, Claire Prada

NOVEMBER 25 2019

Accuracy of Green's function estimation from correlation of diffuse elastic waves on thin plates

Lynda Chehami; Emmanuel Moulin; Julien de Rosny; Claire Prada

J Acoust Soc Am 146, 3505–3511 (2019)
https://doi.org/10.1121/1.5134066

Accuracy of Green's function estimation from correlation of diffuse elastic waves on thin plates

Lynda Chehami,[1,a)] Emmanuel Moulin,[1] Julien de Rosny,[2] and Claire Prada[2]
[1]*Université Polytechnique Hauts-de-France (UPHF), CNRS, Univ. Lille, ISEN, Centrale Lille, UMR 8520-IEMN, DOAE, F-59313 Valenciennes, France*
[2]*Institut Langevin, CNRS, UMR 7587, F-75231 Paris, France*

(Received 17 July 2019; revised 15 October 2019; accepted 28 October 2019; published online 25 November 2019)

In a reverberant cavity, when a noise field is sufficiently diffuse, the correlation of the signal measured by two sensors provides an estimation of the Green's function (GF) between them. Here, the convergence of this passive estimation in the case of elastic waves on thin plates is studied. A statistical approach is proposed, which relates the similarity between the cross correlation and the GF to the structural properties of the plate and the number of uncorrelated sources. The analysis is sustained by experimental results obtained on an aluminum plate. This study allows us to evaluate the efficiency of passive structural health monitoring of plate-like structures based on noise correlation. Finally, a most interesting finding shows an absolute upper bound of the signal-to-noise ratio for GF quality reconstruction: $4N_s/5$, independently of the plate properties. © *2019 Acoustical Society of America*.
https://doi.org/10.1121/1.5134066

[MCR] Pages: 3505–3511

I. INTRODUCTION

Embedded structural health monitoring (SHM) systems offer the prospect of detecting defects at an early stage before serious damage occurs in the structure such as cracks or corrosion in metallic materials or delaminations in composite structures. Pitch-catch is one of the most commonly used techniques based on ultrasonic detection of damage. It consists of analyzing the wave propagation between a source and a sensor. This classical technique generally aims at minimizing the number of sensors to limit the embedded mass as well as the sensors' intrusiveness within the structure and power consumption. In some situations, active methods are not practical or feasible due to environmental restrictions, for example. An alternative way could then consist in using passive techniques taking benefit of the ambient noise to estimate the Green's function (GF). Indeed, since the striking demonstration that the time derivative of the fully diffuse field cross correlation between two points coincides with the difference between the "causal" and "anticausal" impulse responses (GF), argued theoretically and then demonstrated ultrasonically by Lobkis and Weaver,[1] the approach has been successfully used for a variety of applications, including ultrasonics,[1,2] ocean acoustics,[3] and most notably seismology.[4–6] In SHM, however, only a few studies have been devoted to the passive reconstruction of GFs. For example, the possibility of detecting and localizing defects using ambient noise (friction noise, acoustic noise, etc.) more or less uniformly generated on surface plates has been demonstrated numerically and experimentally in recent works.[7–9] Theoretically, if the GF of a finite medium is to be reconstructed using this principle, the field should result from uniformly distributed uncorrelated noise sources. However, in practice, most wave fields only partially fulfill this condition. Hence, it is necessary to know how well cross correlations converge toward the exact GF and the origin of the mismatch in such cases. In complex media (reverberation, multiscattering, etc.), only statistical quantities can be inferred and a mismatch appears as a fluctuation of the cross correlation. In a closed reverberant medium, Weaver and Lobkis[10] studied the mean and variance for the diffuse field correlation functions to predict the fidelity of the passively obtained correlation function to an actively measured waveform. The authors extend their studies later for open systems.[11] More recently, Yoritomo and Weaver[12] focused on the remaining differences between GF and cross correlation due to spurious arrivals from scatterers and/or point sources in unbounded scattering media. Hejazi *et al.*[13] studied the convergence of the cross correlation between parts of the coda, i.e., the parts of the transient response generated by pulsed-like sources. Their obtained results are analyzed through vibrational modes of the plate. The authors show, particularly, that for a large density of sources, an accurate estimation of the GF can be obtained even with a very short part of the coda. Here, we propose to focus our attention on the case of a set of uncorrelated noise sources. This paper is structured as follows. In Sec. I, the proposed statistical model based on the relative noise level (RNL) is introduced. In Sec. II, a quantitative estimation of the RNL is derived. In Sec. III, we show that the derived theoretical expressions are in accord with experiments. Finally, a conclusion is given in Sec. IV.

II. STATISTICAL DESCRIPTION OF THE GF RECONSTRUCTION AND RESIDUAL TERMS

A thin reverberating plate with two point receivers R_i and R_j at its surface and subject to a finite set number of noise sources (N_s) is considered. At each receiver, the recorded wave field can be written as the sum of GF convolved with the source functions $q_k(t)$,

[a)]Electronic mail: lynda.chehami@uphf.fr

$$s_i(t) = \sum_{k=1}^{N_s} G(\mathbf{r}_i, \mathbf{r}_k, t) \otimes q_k(t). \tag{1}$$

$\otimes$ denotes the time convolution. We define the normalized cross correlation

$$C_{ij}(t) = \frac{1}{N_s} s_i(-t) \otimes s_j(t). \tag{2}$$

Under the assumption of uncorrelated noise sources (see Appendix A), the cross correlation can be expressed as

$$C_{ij}(t) = \frac{\Delta T}{N_s} \sum_{k=1}^{N_s} \mathcal{C}_{ij,k}(t), \tag{3}$$

with $\mathcal{C}_{ij,k}(t) = G(\mathbf{r}_i, \mathbf{r}_k, -t) \otimes G(\mathbf{r}_j, \mathbf{r}_k, t) \otimes R(t)$.

The function $R(t)$ is the inverse Fourier transform of the power spectral density, and ΔT is the duration of noise recording. In the following and without loss of generality, ΔT is set to 1. It has been shown in recent works[7] (through modal decomposition of the GF over the eigenvibrational modes of the plate) that the cross correlation of the flexural waves can be expressed as

$$C_{ij}(t) = D_{ij}(t) + n_{ij}(t), \tag{4}$$

where

$$D_{ij}(t) = \frac{\tau_a}{2\mathcal{S}\rho h} \left[G(\mathbf{r}_i, \mathbf{r}_j, t) - G(\mathbf{r}_i, \mathbf{r}_j, -t)\right] \otimes \cdots \otimes \int_{-\infty}^{t} R(\tau)\, \mathrm{d}\tau, \tag{5}$$

with h the plate thickness, ρ the density of the plate material, $\mathcal{S}$ the plate area, and τ_a the attenuation time related to the exponential decay of the reverberated signals. Function $D_{ij}(t)$. represents a deterministic term containing the causal and anticausal parts of the GF between the two receiver locations. Term $n_{ij}(t)$ is the residual noise reconstruction of the GF, also called the *spurious term*. It is shown in previous works[7] that $n_{ij}(t)$ goes toward zero when N_s is sufficiently large. The spurious term can be quantified by the ratio of energy between the residue of correlation $n_{ij}(t)$ and the deterministic part $D_{ij}(t)$, denoted by RNL. Since we are interested here in an average behavior, we define the expected value of this energy ratio as

$$\mathrm{RNL}(N_s) = \frac{\int_{-\infty}^{\infty} \mathrm{Var}\left[C_{ij}(t)\right] \mathrm{d}t}{\int_{-\infty}^{\infty} D_{ij}^2(t)\, \mathrm{d}t}, \tag{6}$$

where Var is defined as

$$\mathrm{Var}\left[C_{ij}(t)\right] = \langle C_{ij}^2(t)\rangle - \langle C_{ij}(t)\rangle^2. \tag{7}$$

Notation "$\langle . \rangle$" denotes the statistical averaging over the noise sources positions. Because the statistical distribution of the source position is assumed to be uniform, $\langle . \rangle$ reduces to a continuous average over the plate surface. We note that $\langle C_{ij}(t)\rangle = D_{ij}(t)$ because $\langle n_{ij}\rangle = 0$ [see Eq. (5) in Ref. 7 for more details]. This result is intuitive because $\langle C_{ij}(t)\rangle$ can be interpreted as if the correlation is estimated from a uniform and dense distribution of noises sources. In such a case, the cross correlation converges perfectly toward the GF. In this case, and by introducing Eq. (3) into Eq. (7),

$$\mathrm{Var}\left[C_{ij}(t)\right] = \frac{1}{N_s^2} \left\langle \left(\sum_{k=1}^{N_s} \mathcal{C}_{ij,k}(t) \right)^2 \right\rangle - D_{ij}^2(t). \tag{8}$$

Separating into double sum above the terms with $k = l$ and the cross terms, and introducing Eq. (8) into Eq. (6), the RNL can be written as

$$\mathrm{RNL}(N_s) = \frac{\int_{-\infty}^{\infty} \sum_{k=1}^{N_s} \langle \mathcal{C}_{ij,k}^2(t)\rangle \, \mathrm{d}t}{N_s^2 \int_{-\infty}^{\infty} D_{ij}^2(t)\, \mathrm{d}t} - 1 + \frac{\int_{-\infty}^{\infty} \sum_{k=1,l\neq k}^{N_s,N_s} \langle \mathcal{C}_{ij,k}(t)\, \mathcal{C}_{ij,l}(t)\rangle \, \mathrm{d}t}{N_s^2 \int_{-\infty}^{\infty} D_{ij}^2(t)\, \mathrm{d}t}. \tag{9}$$

Here, we consider that the sources are randomly distributed over the plate surface and sufficiently distant ($>\lambda/2$), such as $\mathcal{C}_{ij,k}(t)$ and $\mathcal{C}_{ij,l}(t)$ can be considered as independent for $k \neq l$. Consequently, $\langle \mathcal{C}_{ij,k}(t)\, \mathcal{C}_{ij,l}(t)\rangle = \langle \mathcal{C}_{ij,k}(t)\rangle \langle \mathcal{C}_{ij,l}(t)\rangle = D_{ij}^2(t)$. Equation (9) becomes

$$\mathrm{RNL}(N_s) = \frac{\int_{-\infty}^{\infty} N_s \langle \mathcal{C}_{ij,k}^2(t)\rangle \, \mathrm{d}t}{N_s^2 \int_{-\infty}^{\infty} D_{ij}^2(t)\, \mathrm{d}t} - 1 + \frac{\int_{-\infty}^{\infty} N_s\,(N_s - 1)\, D_{ij}^2(t) \mathrm{d}t}{N_s^2 \int_{-\infty}^{\infty} D_{ij}^2(t)\, \mathrm{d}t}. \tag{10}$$

Using the Parseval's theorem, the RNL expression given in Eq. (10) simplifies into

$$\mathrm{RNL}(N_s) = \frac{1}{N_s}(A - 1), \tag{11}$$

with

$$A = \frac{\int_{\Delta\omega} \langle |\tilde{\mathcal{C}}_{ij,k}(\omega)|^2\rangle \, \mathrm{d}\omega}{\int_{\Delta\omega} |\tilde{D}_{ij}(\omega)|^2 \, \mathrm{d}\omega}, \tag{12}$$

where $\Delta\omega$ is the frequency band, and the tilde symbol above a function refers to the Fourier transform of this last.

Taking the Fourier transform of Eq. (5) yields

$$\tilde{D}_{ij}(\omega) = 2j\,\Im\tilde{G}(\mathbf{r}_i, \mathbf{r}_j, \omega) \frac{\tilde{R}(\omega)\,\tau_a}{2j\,\omega\,\rho\,h\,\mathcal{S}}, \tag{13}$$

where $\tilde{R}(\omega)$ stands for the noise spectral density. The function $\Im\tilde{G}(\mathbf{r}_i,\mathbf{r}_j,\omega)$ is the imaginary part of the GF that can be expressed in terms of eigen-modes

$$\Im\tilde{G}(\mathbf{r}_i,\mathbf{r}_j,\omega)=\frac{\omega}{\rho\,h\,\tau_a}\sum_n \phi_n(\mathbf{r}_i)\,\phi_n(\mathbf{r}_j)\tilde{f}(\omega,\omega_n),$$

with $\tilde{f}(\omega,\omega_n)=[(\omega^2-\omega_n^2)^2+(\omega/\tau_a)^2]^{-1}$, and $\phi_n(\mathbf{r})$ is the eigen-mode at angular frequency ω_n.

Here, we are interested in quantifying term A in average, independently of the positions of a particular receivers pair. To that end, we introduce $\{.\}$, the averaging value over all the receiver positions.

$$\begin{aligned}\{|\tilde{D}_{ij}(\omega)|^2\}=\frac{|\tilde{R}(\omega)|^2}{\rho^4 h^4\mathcal{S}^2}\Big[&\sum_n\{\phi_n^2(\mathbf{r}_i)\}\{\phi_n^2(\mathbf{r}_j)\}\\&\times\tilde{f}^2(\omega,\omega_n)+\cdots+\sum_{n,n\neq n'}\{\phi_n(\mathbf{r}_i)\phi_{n'}(\mathbf{r}_i)\}\\&\times\{\phi_n(\mathbf{r}_j)\phi_{n'}(\mathbf{r}_j)\}\cdots\tilde{f}(\omega,\omega_n)\tilde{f}(\omega,\omega_{n'})\Big].\end{aligned}\tag{14}$$

By the orthogonality of modes, we have $\{\phi_n(\mathbf{r}_i)\phi_{n'}(\mathbf{r}_i)\}=\delta_{n,n'}/\mathcal{S}$, where $\delta_{n,n'}$ is Kronecker's symbol.

Equation (14) becomes

$$\{|\tilde{D}_{ij}(\omega)|^2\}=\frac{|\tilde{R}(\omega)|^2}{\rho^4 h^4\mathcal{S}^4}\sum_n\tilde{f}^2(\omega,\omega_n).\tag{15}$$

The discrete sum $\sum_n\tilde{f}^2(\omega,\omega_n)$ is derived in Appendix B. It depends on the modal density that is constant for a plate with respect to ω' and equal to[14]

$$\eta_0=\frac{\mathcal{S}}{4\pi}\sqrt{\frac{\rho\,h}{\mathcal{D}}},\tag{16}$$

where the plate flexural stiffness $\mathcal{D}$ is given by $E\,h^3/12\,(1-\nu^2)$.[14]

Finally, Eq. (15) is given by

$$\{|\tilde{D}_{ij}(\omega)|^2\}\simeq\beta\,\eta_0\,\pi\,\tau_a^3,\tag{17}$$

with $\beta=|\tilde{R}(\omega)|^2/4\,\omega^4\,(\rho\,h\,\mathcal{S})^4$.

Similarly, we can deduce $\langle\{|\tilde{C}_{ij,k}(\omega)|^2\}\rangle$. The derivation is given in Appendix C. An expression of RNL for a chaotic shape plate is also derived. This corresponds to the state in which the multiple reflected waves will reach after a given time (mixing time), any point in the medium without any privileged direction with random phases and amplitudes. In this particular case, it is shown that the eigen-modes of the plate obey the Gaussian statistic, which allows us to write $\langle\phi^4\rangle=3\,\langle\phi^2\rangle$. Its expression is given in Appendix C. From Eqs. (17) and (C14), and replacing by the expression of modal density given in Eq. (16), we deduce the final expression of the parameter A for a rectangular and chaotic plate, respectively.

$$A=\alpha+\pi\frac{\eta_0}{\tau_a},\tag{18}$$

with $\alpha=9/4$ for the rectangular plate, and $\alpha=3$ for the chaotic plate.

Consequently, the parameter A depends only on the structural parameters of the plate. Inserting Eq. (18) into Eq. (11), the final analytic expression of the RNL is

$$\mathrm{RNL}(N_s)=\frac{1}{N_s}\left(\alpha-1+\pi\,\frac{\eta_0}{\tau_a}\right).\tag{19}$$

As a consequence, for accurate retrieval of a GF, the reconstruction error must diminish when increasing the number of sources N_s, the damping time τ_a, and small plate area. One interesting result is that optimal reconstruction quality would be achieved for negligible attenuation ($\tau_a\gg\eta_0$). In that case, RNL $\simeq(\alpha-1)/N_s$, which implies the existence of a lower bound of the RNL, equals $5/4\,N_s$ and $2/N_s$ for the rectangular and the chaotic plate, respectively.

III. EXPERIMENTAL VALIDATION AND DISCUSSION

Experiments are conducted in a thin rectangular aluminum plate of $0.5\times0.6\,\mathrm{m}^2$ and 3 mm thick, with six piezoelectric transducers attached to one side of the plate (see Fig. 1).

Instead of a short pulse, a linear chirp (0.8 V amplitude, 1.5 s of duration) in the frequency band of 100 Hz to 40 kHz is sent via these transducers in order to improve the signal-to-noise ratio. On the other side of the plate, velocity induced by

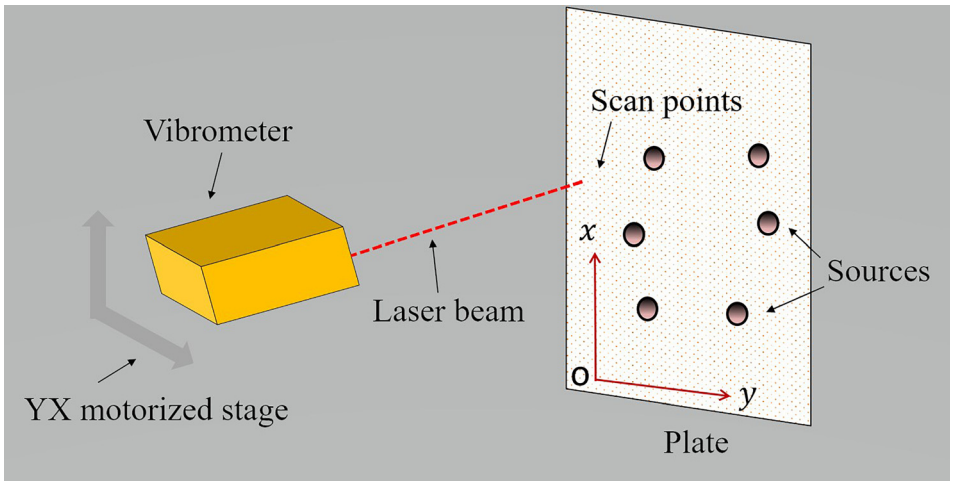

FIG. 1. (Color online) Experimental setup described in Sec. III. Six piezoelectric transducers are glued on one plate surface at positions (19.4,25.6) cm, (29.7,21.3) cm, (35,27.8) cm, (32.5,34.7) cm, (27,42.4) cm, (20.7,37.6) cm (the origin is taken at the left bottom corner of the plate). Velocity scans are performed on a grid of roughly 304 regularly spaced locations on the other side of the plate.

the vibration (flexural waves) is scanned with a laser vibrometer mounted on a two axis stepping motor bench. Velocity scans are performed on a grid of roughly 304 regularly spaced locations (with a uniform distance of 3 cm between 2 points along the x and y plate directions). The signals are digitized over 24 bits at a sample rate of 96 kS/s (MOTU 24 I/O, Cambridge, MA). Each recorded signal is cross correlated with the emitted chirp to extract the impulse response. Consequently, the emission impulsion $q(t)$ is the autocorrelation of the chirp. The envelope of the reverberated signals shows exponential decay. The averaged envelope of the reverberated signals while removing the direct paths of propagation (to keep only the reverberant part) is plotted in Fig. 2 in logarithmic scale.

By fitting an exponential function according to $e^{-t/2\tau_a}$ to the averaged envelope of the reverberated signals, an attenuation time $\tau_a = 6$ ms is found, which is approximately the modal density of the plate (5 ms). Now, thanks to the reciprocity of acoustic waves, the measured signals can be considered as resulting in a virtual source emitting at the scanned point locations, and virtually recorded at transducer locations. This allows to study the RNL as a function of a wide variety of source distributions. The virtual sources created by reciprocity are sufficiently distant (approximately one wavelength at 20 kHz). For each source position, an experiment is performed. From N_s experiment runs, we obtain the $N_s \times N_R$ transient normal responses (here N_s refers to the 304 virtual sources, and N_R refers to the 6 receivers) $s_{ik}(t)$ (i and k stand for index of receiver and source, respectively). From this set of signals, we directly estimate the cross correlations for each receiver pair (R_i,R_j), $s_{ik}(t) \otimes s_{jk}(-t)$, then we sum over sources according to Eq. (20),

$$C_{ij}(t) = \frac{1}{N_s} \sum_{k=1}^{N_s} s_{ik}(t) \otimes s_{jk}(-t). \tag{20}$$

Since $s_{ik}(t) = G(\mathbf{r}_i, \mathbf{r}_k, t) \otimes q_k(t)$, this expression is equivalent to Eq. (3) assuming that the noise autocorrelation is equal to $q(t) \otimes q(-t)$. In this way, we simulate a situation similar to that of uncorrelated noise sources. The experimental RNL is plotted and compared to the theory, i.e., Eq. (19) in Fig. 3 as a function of the number of "noise" sources. The error bars are estimated from the fluctuations of the RNL with respect to the receiver positions (6 arbitrary combinations are considered among the 15 total number of cases choosing 2 receivers from 6 receivers).

The small error bars show the weak influence of the receiver positions on the relative noise ratio, and favorably compared to the theory [Eq. (19)].

We can distinguish three regimes with respect to N_s. First, for small values of point sources $N_s < 5$ the spurious term $n_{ij}(t)$ is dominant (RNL > 1), which means that the GF is drowned in the residual noise. Second, for $5 \leq N_s < 100$, the RNL holds with the theoretical prediction. Finally, for high number of sources $N_s > 100$, the relative noise ratio deviates from the theoretical estimate. Actually, the mismatch for a higher number of sources comes from the experimental estimation of $D_{ij}(t)$. Indeed, $D_{ij}(t)$ is assumed to be exactly equal to the sum of the correlation when all the available point virtual sources M_s (here $M_s = 304$) are taken into account. This assumption is only partially true. One can show that with such a definition of the asymptotic value of the cross correlation, the theoretical expression of this new definition of RNL, RNL′, is actually given by

$$\mathrm{RNL}'(N_s) = \left(\frac{1}{N_s} - \frac{1}{M_s}\right)\left(\alpha - 1 + \pi\frac{\eta_0}{\tau_a}\right). \tag{21}$$

Note that, by definition, when N_s reaches M_s, the RNL is equal to 0. This new expression RNL′ follows very well to experimental data. Based on this study, it appears that the behavior of the convergence of noise correlation toward the GF behaves quite differently in the case of three-dimensional elastic solids.[10] In such a case, the number of sources required to get the same quality of reconstruction scales with the square of the central frequency of noise. Here, we have seen that the RNL is independent of the frequency.

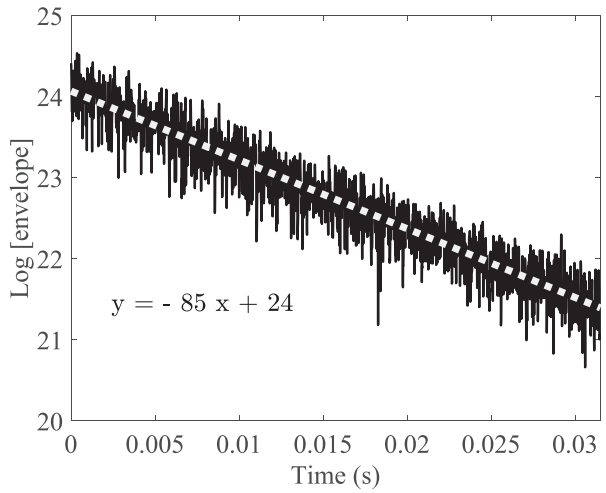

FIG. 2. Estimation of the attenuation time for an aluminum plate of 50×60 cm^2 and 3 mm thick. By fitting an exponential function (dashed line) according to $e^{-t/2\tau_a}$ to the averaged envelope of the reverberated signals (solid line), an attenuation time $\tau = 1/85 \simeq 12$ ms ($\tau_a = \tau/2 = 6$ ms), is estimated.

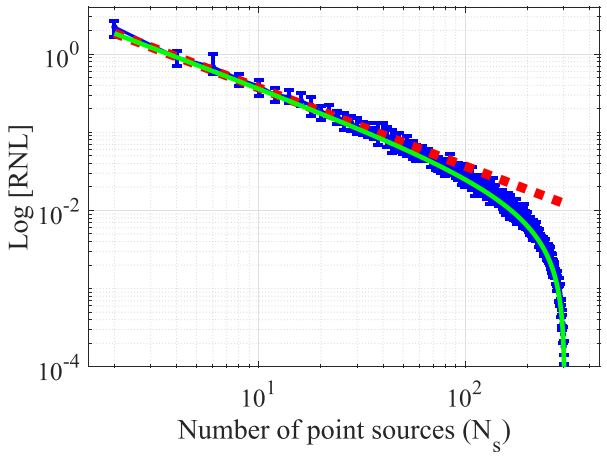

FIG. 3. (Color online) Averaged RNL (log scale) over six receiver pairs as a function of the number of sources N_s derived from experimental data (error bars curve) using Eq. (6), and modeled (dashed line) based on Eq. (19) compared to Eq. (21) (solid line). An error bar is computed for each six couples of receivers.

IV. CONCLUSION

Here, we have considered a quasi-diffuse uniform flexural wave field due to a random distribution of uncorrelated point sources in a thin plate. Given any receiver pair, the transient response can be reconstructed experimentally by cross correlation of diffused fields. We have also derived expressions for the relative noise ratio as functions of the number of point sources [Eq. (19)]. Laboratory experiments are conducted and favorably compared to the theoretical estimates. Through statistical modal analysis, we find that the estimation of the GF will be better when (i) the number of sources is larger, (ii) the plate absorption is smaller, and (iii) the plate is larger. Equation (19) summarizes these results for rectangular and chaotic plates. Finally, a most interesting finding shows an absolute upper bound of the signal-to-noise ratio (the inverse of RNL) that is $4N_s/5$, independently of the plate properties.

ACKNOWLEDGMENTS

This work has been supported by the French National Research Agency (ANR), Grant No. ANR2011 BS0903901, PASNI Project.

APPENDIX A: COMPARAISON OF THE CORRELATION OF THE FIELD GENERATED BY DECORRELATED NOISE SOURCES AND PULSED SOURCES

1. Noise correlation

Inserting Eq. (A4) in Eq. (2), the correlation of the field generated by N_s sources of noise is expressed as

$$C_{ij}(t)=\frac{1}{N_s}\sum_{k=1,l=1}^{N_s,N_s} G(\mathbf{r}_i,\mathbf{r}_k,t)\otimes G(\mathbf{r}_i,\mathbf{r}_l,-t)\otimes q_k(t)\otimes q_l(-t). \tag{A1}$$

Assuming that the cross correlation is computed over a sufficiently large time window of duration ΔT, the cross correlation of the signal emitted by two decorrelated noise sources at positions $\mathbf{r}_k$ and $\mathbf{r}_l$ obeys to

$$q_k(t)\otimes q_l(-t)\approx \delta_{k,l}\Delta T R(t), \tag{A2}$$

where $R(t)$ is the inverse Fourier transform of the power spectral density of the noise source, and $\delta_{k,l}$ is the Kronecker symbol.

Combining the two last relations, the noise correlation is given by

$$C_{ij}(t)=\frac{\Delta T}{N_s}\sum_{k=1}^{N_s} G(\mathbf{r}_i,\mathbf{r}_k,t)\otimes G(\mathbf{r}_i,\mathbf{r}_k,-t)\otimes R(t). \tag{A3}$$

2. Pulse correlation

Now let us assume that a pulse $e(t)$ is emitted at position $\mathbf{r}_k$. The transient response recorded at position $\mathbf{r}_i$ can be written in terms of a GF as

$$s'_{i,k}(t)=G(\mathbf{r}_i,\mathbf{r}_k,t)\otimes e(t). \tag{A4}$$

Based on the transient responses between all sources and receivers, one can compute the following correlation:

$$C'_{ij}(t)=\frac{1}{N_s}\sum_{k=1}^{N_s} s'_{i,k}(t)\otimes s'_{j,k}(-t). \tag{A5}$$

This last correlation can be expressed as

$$C'_{ij}(t)=\frac{1}{N_s}\sum_{k=1}^{N_s} G(\mathbf{r}_i,\mathbf{r}_k,t)\otimes G(\mathbf{r}_j,\mathbf{r}_k,-t)\otimes e(t)\otimes e(-t). \tag{A6}$$

3. Comparison

Assuming the spectral power density of the noise to be proportional to the power spectrum of the pulse, the noise cross correlation $C_{ij}(t)$ is proportional to the pulse cross correlation. As a consequence, the correlation of uncorrelated noise sources can be approximated by the sum of correlations of pulse sources given by Eq. (A5).

APPENDIX B: EVALUATION OF DISCRETE SUM

Knowing the modal density of the plate $\eta(\omega)$, a reasonable approximation of a discrete sum over a function g that depends on the eigenmodes is

$$\sum_n g(\omega_n)\simeq\int_0^\infty g(\omega)\eta(\omega')\,\mathrm{d}\omega'. \tag{B1}$$

Because the plate density does not depend on the frequency, the previous expression can be simplified into

$$\sum_n g(\omega_n)\simeq\eta_0\int_0^\infty g(\omega')\,\mathrm{d}\omega'. \tag{B2}$$

1. Evaluation of $\sum_n \tilde{f}^2(\omega,\omega_n)$

Applying this result to the case $g(\omega')=\tilde{f}^2(\omega,\omega')$, it comes

$$\sum_n \tilde{f}^2(\omega,\omega_n) \simeq \eta_0\int_0^\infty \frac{1}{\left[((\omega-\omega')(\omega+\omega'))^2+\left(\frac{\omega}{\tau_a}\right)^2\right]^2}\,\mathrm{d}\omega'. \tag{B3}$$

We can show that $\tilde{f}(\omega,\omega')$ is negligible only outside a narrow interval around ω. So, it becomes

$$\sum_n \tilde{f}^2(\omega,\omega_n)\simeq\eta_0\int_0^\infty \frac{1}{\omega^4\left[4(\omega'-\omega)^2+\left(\frac{1}{\tau_a}\right)^2\right]^2}\,\mathrm{d}\omega'. \tag{B4}$$

Employing Eq. (B2) with $g(\omega') = \tilde{f}(\omega, \omega')$, and by taking $u = \omega' - \omega$ and $z = 1/2\tau_a$ it becomes

$$\sum_n \tilde{f}(\omega, \omega_n) \simeq \frac{\eta_0}{4\omega^2} \int_{-\infty}^{\infty} \frac{1}{(u^2 + z^2)}\, \mathrm{d}u. \tag{B5}$$

So, Eq. (B4) becomes

$$\sum_n \tilde{f}^2(\omega, \omega_n) \simeq \frac{\eta_0}{16\omega^4} \int_{-\infty}^{\infty} \frac{1}{(u^2 + z^2)^2}\, \mathrm{d}u. \tag{B6}$$

Because $\int_{-\infty}^{\infty} 1/(u^2 + z^2)^2\, \mathrm{d}u \simeq \pi/2\, z^3$, it becomes

$$\sum_n \tilde{f}^2(\omega, \omega_n) \simeq \frac{\eta_0 \pi \tau_a^3}{4\omega^4}. \tag{B7}$$

The approximation above is checked numerically by computing the plate's vibration modes considering aluminum material properties used in experiments (see Fig. 4). As can be observed, the approximated and theoretical curves are in a good agreement at low frequencies up to 40 kHz, which is the working frequency band considered for the experiments.

2. Evaluation of $\sum_n \tilde{f}(\omega, \omega_n)$

Employing Eq. (B2) with $g(\omega') = \tilde{f}(\omega, \omega')$ and the same approximations used to go from Eq. (B3) to Eq. (B6), it becomes

$$\sum_n \tilde{f}(\omega, \omega_n) \simeq \frac{\eta_0}{4\omega^2} \int_{-\infty}^{\infty} \frac{1}{(u^2 + z^2)}\, \mathrm{d}u, \tag{B8}$$

with $z = 1/2\tau_a$.

Because $\int_{-\infty}^{\infty} 1/(u^2 + z^2)\, \mathrm{d}u = \pi/z$, it becomes

$$\sum_n \tilde{f}(\omega, \omega_n) \simeq \frac{\pi}{2} \frac{\eta_0 \tau_a}{\omega^2}. \tag{B9}$$

APPENDIX C: EVALUATION OF $\langle\{|\tilde{\mathcal{C}}_{ij,k}(\omega)|^2\}\rangle$

We have

$$\tilde{\mathcal{C}}_{ij,k}(\omega) = \tilde{G}^*(\mathbf{r}_i, \mathbf{r}_k, \omega)\, \tilde{G}(\mathbf{r}_j, \mathbf{r}_k, \omega)\, \tilde{R}(\omega). \tag{C1}$$

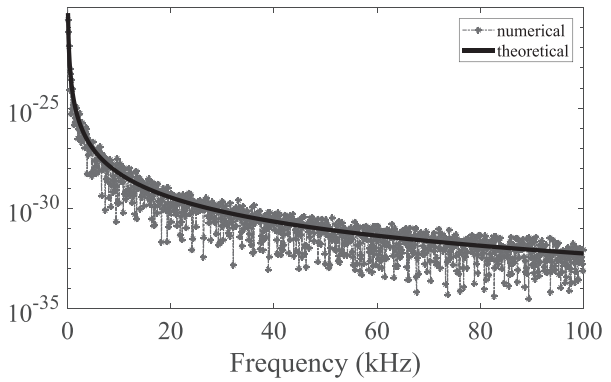

FIG. 4. Numerical computing of $\sum_n \tilde{f}^2(\omega, \omega_n)$ (dashed line) compared to the theoretical approximation given by Eq. (B7) (solid line) in frequency band [0 100] kHz in logarithmic scale.

Taking the averaging value over all the receiver positions (denoted by $\{.\}$), and assuming statistical independence of $\tilde{G}_{r_i,r_k}(\omega)$ and $\tilde{G}_{r_j,r_k}(\omega)$ yields

$$\{|\tilde{\mathcal{C}}_{ij,k}(\omega)|^2\} = \{|\tilde{G}(\mathbf{r}, \mathbf{r}_k, \omega)|^2\}^2\, |\tilde{R}(\omega)|^2, \tag{C2}$$

with

$$\tilde{G}(\mathbf{r}, \mathbf{r}_k, \omega) = \frac{1}{\rho\, h} \sum_n \frac{\phi_n(\mathbf{r}_k)\phi_n(\mathbf{r})}{(\omega^2 - \omega_n^2) - j\, \dfrac{\omega}{\tau_a}}. \tag{C3}$$

Inserting Eq. (C3) into Eq. (C2) and separating into double sum the terms $n = n'$ and the crossed terms, yields

$$\begin{aligned}\{|\tilde{\mathcal{C}}_{ij,k}(\omega)|^2\} = \frac{|\tilde{R}(\omega)|^2}{(\rho\, h)^4} \Bigg[& \sum_n \phi_n^2(\mathbf{r}_k)\{\phi_n^2(\mathbf{r})\} \bar{f}(\omega, \omega_n) \\ & + \sum_n \sum_{n \neq n'} \phi_n(\mathbf{r}_k)\, \phi_{n'}(\mathbf{r}_k) \{\phi_n(\mathbf{r})\phi_{n'}(\mathbf{r})\} \\ & \times \tilde{g}(\omega, \omega_n)\tilde{g}^*(\omega, \omega_{n'})\Bigg]^2,\end{aligned} \tag{C4}$$

with

$$\tilde{g}(\omega, \omega_n) = \left[(\omega^2 - \omega_n^2) - j\, \frac{\omega}{\tau_a}\right]^{-1}. \tag{C5}$$

By the orthogonality of modes, we have $\{\phi_n(\mathbf{r})\phi_{n'}(\mathbf{r})\} = \delta_{n,n'}/\mathcal{S}$, where $\delta_{n,n'}$ is Kronecker's symbol, it becomes

$$\left\{|\tilde{\mathcal{C}}_{ij,k}(\omega)|^2\right\} = \frac{|\tilde{R}(\omega)|^2}{\rho^4\, h^4\, \mathcal{S}^2} \left[\sum_m \phi_m^2(rk) \bar{f}(\omega, \omega_n)\right]^2. \tag{C6}$$

By separating into double sum the terms $n = n'$ and the crossed terms, and averaging over the source positions $\langle\cdot\rangle$, it becomes

$$\left\langle \left\{|\tilde{\mathcal{C}}_{ij,k}(\omega)|^2\right\} \right\rangle = \frac{|\tilde{R}(\omega)|^2}{\rho^4\, h^4\, \mathcal{S}^2}\, (I_1 + I_2), \tag{C7}$$

with

$$\begin{aligned} I_1 &= \sum_n \langle \phi_n^4(\mathbf{r}_k) \rangle \tilde{f}^2(\omega, \omega_n)\,, \\ I_2 &= \sum_n \sum_{n \neq n'} \langle \phi_n^2(\mathbf{r}_k) \phi_{n'}^2(\mathbf{r}_k) \rangle \tilde{f}(\omega, \omega_n) \tilde{f}(\omega, \omega_{n'}). \end{aligned} \tag{C8}$$

Using the classical result derived from the statistical energy analysis of modes of coefficient α defined as[15] and also the fact that in the case of chaotic eigenstates, the spatial averaging can be approximated by the ensemble averaging,[16] it becomes

$$\alpha = \frac{\langle \phi_n^4(\mathbf{r}_k) \rangle}{\langle \phi_n^2(\mathbf{r}_k) \rangle^2} = \begin{cases} \left(\dfrac{3}{2}\right)^d & (\text{rectangular plate}), \\ 3 & (\text{chaotic plate}), \end{cases} \tag{C9}$$

with d the medium dimension (here, $d = 2$ for the case of the plate).

We recall that $\langle \phi_n^2 \rangle = 1/\mathcal{S}$, we deduce then $\langle \phi_n^4(\mathbf{r}_k) \rangle \simeq 3(1/\mathcal{S}^2)$ for the chaotic plate. Using Eq. (B7), the final expression of I_1 is

$$I_1 = \alpha \left(\frac{1}{\mathcal{S}^2}\right) \sum_n \tilde{f}^2(\omega, \omega_n) = \alpha \left(\frac{1}{\mathcal{S}^2}\right) \frac{\eta_0 \, \pi \, \tau_a^3}{4 \, \omega^4}. \quad \text{(C10)}$$

Considering the statistical independence of $\langle \phi_n^2(\mathbf{r}_k) \, \phi_{n'}^2(\mathbf{r}_k) \rangle$ and modes orthogonality property for both cases, rectangular plate and chaotic plate, we have $\langle \phi_n^2(\mathbf{r}_k) \, \phi_{n'}^2(\mathbf{r}_k) \rangle = 1/\mathcal{S}^2, \ \forall n \neq n'$,

$$I_2 = \frac{1}{\mathcal{S}^2} \sum_n \tilde{f}(\omega, \omega_n) \sum_{n \neq n'} \tilde{f}(\omega, \omega_{n'}) \quad \text{(C11)}$$

$$\approx \frac{1}{\mathcal{S}^2} \left(\sum_n \tilde{f}(\omega, \omega_n) \right)^2. \quad \text{(C12)}$$

From the derivation of the right-hand term in Appendix B, it becomes

$$I_2 = \frac{1}{\mathcal{S}^2} \left(\frac{\pi}{2} \frac{\eta_0 \tau_a}{\omega^2} \right)^2. \quad \text{(C13)}$$

From Eqs. (C10) and (C13), we deduce the final expression of the term $\langle \{ |\tilde{\mathcal{C}}_{ij,k}(\omega)|^2 \} \rangle$,

$$\langle \{ |\tilde{\mathcal{C}}_{ij,k}(\omega)|^2 \} \rangle = \beta \left[\alpha \, \eta_0 \, \pi \, \tau_a^3 + \pi^2 \, \eta_0^2 \, \tau_a^2 \right], \quad \text{(C14)}$$

with $\beta = |\tilde{R}(\omega)|^2 / 4 \, \omega^4 \, (\rho \, h \, \mathcal{S})^4$, and $\alpha = \frac{9}{4}$ (respectively, $\alpha = 3$) for the rectangular (respectively, chaotic) plate.

[1]O. I. Lobkis and R. L. Weaver, "On the emergence of the Green's function in the correlations of a diffuse field," J. Acoust. Soc. Am. **110**, 3011–3017 (2001).
[2]R. L. Weaver and O. I. Lobkis, "Ultrasonics without a source: Thermal fluctuation correlations at MHz frequencies," Phys. Rev. Lett. **87**, 134301 (2001).
[3]P. Roux, W. A. Kuperman, and NAPL Group, "Extracting coherent wave fronts from acoustic ambient noise in the ocean," J. Acoust. Soc. Am. **116**, 1995–2003 (2004).
[4]P. Boué, P. Poli, M. Campillo, and P. Roux, "Reverberations, coda waves and ambient noise: Correlations at the global scale and retrieval of the deep phases," Earth Planet. Sci. Lett. **391**, 137–145 (2014).
[5]M. Campillo, P. Roux, B. Romanowicz, and W. Dziewonski, "Seismic imaging and monitoring with ambient noise correlations," Treat. Geophys. **1**, 256–271 (2014).
[6]L. Boschi and C. Weemstra, "Stationary-phase integrals in the cross-correlation of ambient noise," Rev. Geophys. **53**, 411–451, https://doi.org/10.1002/2014RG000455 (2015).
[7]L. Chehami, E. Moulin, J. de Rosny, C. Prada, O. Bou Matar, F. Benmeddour, and J. Assaad, "Detection and localization of a defect in a reverberant plate using acoustic field correlation," J. Appl. Phys. **115**(10), 104901 (2014).
[8]L. Chehami, J. de Rosny, C. Prada, E. Moulin, and J. Assaad, "Experimental study of passive defect localization in plates using ambient noise," IEEE Trans. Ultrason., Ferroelectr., Freq. Control **62**(8), 1544–1553 (2015).
[9]L. Chehami, E. Moulin, J. de Rosny, C. Prada, E. Chatelet, G. Lacerra, K. Gryllias, and F. Massi, "Nonlinear secondary noise sources for passive defect detection using ultrasound sensors," J. Sound. Vib. **386**, 283–294 (2017).
[10]R. L. Weaver and O. I. Lobkis, "The mean and variance of diffuse field correlations in finite bodies," J. Acoust. Soc. Am. **118**, 3447–3456 (2005).
[11]R. L. Weaver and O. I. Lobkis, "Diffuse fields in open systems and the emergence of the Green's function," J. Acoust. Soc. Am. **116**, 2731–2734 (2005).
[12]J. Yoritomo and R. L. Weaver, "Fluctuations in the cross-correlation for fields lacking full diffusivity: The statistics of spurious features," J. Acoust. Soc. Am. **140**, 702–713 (2016).
[13]A. Hejazi Nooghabi, L. Boschi, P. Roux, and J. de Rosny, "Coda reconstruction from cross-correlation of a diffuse field on thin elastic plates," Phys. Rev. E **96**, 032137 (2017).
[14]A. W. Leissa, *Vibration of Plates* (Scientific and Technical Information Division, National Aeronautics and Space Administration, Washington, DC, 1969), Vol. 160, p. 362.
[15]V. Cotoni, R. S. Langley, and M. R. F. Kidner, "Numerical and experimental validation of variance prediction in the statistical energy analysis of built-up systems," J. Sound. Vib. **288**, 701–728 (2005).
[16]M. Srednicki and F. Stiernelof, "Gaussian fluctuations in chaotic eigenstates," J. Phys. A **29**, 5817–5826 (1996).